

HS 0139+0559, HS 0229+8016, HS 0506+7725, and HS 0642+5049: four new long-period cataclysmic variables^{*,**}

A. Aungwerojwit¹, B. T. Gänsicke¹, P. Rodríguez-Gil^{1,2}, H.-J. Hagen³, E. T. Harlaftis⁴, C. Papadimitriou^{5,6},
H. Lehto^{7,8}, S. Araujo-Betancor⁹, U. Heber¹⁰, R. E. Fried¹¹, D. Engels³, and S. Katajainen⁸

¹ Department of Physics, University of Warwick, Coventry CV4 7AL, UK
e-mail: A. Aungwerojwit@warwick.ac.uk

² Instituto de Astrofísica de Canarias, 38200 La Laguna, Tenerife, Spain

³ Hamburger Sternwarte, Universität Hamburg, Gojenbergsweg 112, 21029 Hamburg, Germany

⁴ Institute of Space Applications and Remote Sensing, National Observatory of Athens, PO Box 20048, Athens 11810, Greece

⁵ Institute of Astronomy and Astrophysics, National Observatory of Athens, PO Box 20048, Athens 11810, Greece

⁶ Department of Astrophysics, Astronomy and Mechanics, University of Athens, 157 84 Zografos, Athens, Greece

⁷ Department of Physics, 20014 University of Turku, Finland

⁸ Tuorla Observatory, University of Turku, 21500 Piikkiö, Finland

⁹ Space Telescope Science Institute, 3700 San Martin Drive, Baltimore, MD21218, USA

¹⁰ Astronomisches Institut der Universität Erlangen, Germany

¹¹ Braeside Observatory, PO Box906, Flagstaff, AZ 86002, USA

Received 23 December 2004 / Accepted 3 July 2005

ABSTRACT

We present time-resolved optical spectroscopy and photometry of four relatively bright ($V \sim 14.0\text{--}15.5$) long-period cataclysmic variables (CVs) discovered in the Hamburg Quasar Survey: HS 0139+0559, HS 0229+8016, HS 0506+7725, and HS 0642+5049. Their respective orbital periods, 243.69 ± 0.49 min, 232.550 ± 0.049 min, 212.7 ± 0.2 min, and 225.90 ± 0.23 min are determined from radial velocity and photometric variability studies. HS 0506+7725 is characterised by strong Balmer and He emission lines, short-period ($\sim 10\text{--}20$ min) flickering, and weak X-ray emission in the ROSAT All Sky Survey. The detection of a deep low state ($B \approx 18.5$) identifies HS 0506+7725 as a member of the VY Scl stars. HS 0139+0559, HS 0229+8016, and HS 0642+5049 display thick-disc like spectra and no or only weak flickering activity. HS 0139+0559 and HS 0229+8016 exhibit clean quasi-sinusoidal radial velocity variations of their emission lines but no or very little orbital photometric variability. In contrast, we detect no radial velocity variation in HS 0642+5049 but a noticeable orbital brightness variation. We identify all three systems either as UX UMa-type novalike variables or as Z Cam-type dwarf novae. Our identification of these four new systems underlines that the currently known sample of CVs is rather incomplete even for bright objects. The four new systems add to the clustering of orbital periods in the 3–4 h range found in the sample of HQS selected CVs, and we discuss the large incidence of magnetic CVs and VY Scl/SW Sex stars found in this period range among the known population of CVs.

Key words. stars: binaries: close – stars: individual: HS 0139+0559 – stars: individual: HS 0229+8016 – stars: dwarf novae – stars: individual: HS 0506+7725 – stars: individual: HS 0642+5049 – stars: novae, cataclysmic variables

1. Introduction

Standard models for the population of cataclysmic variables (CVs) predict that the vast majority of all CVs should have

short orbital periods, $P_{\text{orb}} < 2$ h (e.g. Kolb 1993; Howell et al. 1997), and a space density of $2 \times 10^{-5}\text{--}2 \times 10^{-4}$ pc⁻³ (Ritter & Burkert 1986; de Kool 1992; Politano 1996). These predictions contrast with the properties of the observed population of galactic CVs, with an estimated space density of $\sim 6 \times 10^{-6}$ pc⁻³ (Ringwald 1996; Araujo-Betancor et al. 2005b) and an apparent lack of short-period systems. Possible reasons for these discrepancies are uncertainties in the theory of CV evolution (e.g. King 1988; Schenker & King 2002; Andronov et al. 2003; Barker & Kolb 2003; Taam et al. 2003), but also observational selection effects in the known CV population (e.g. Downes 1986; Ringwald 1996; Gänsicke 2005).

About 75% of all known CVs have been discovered either because of their variability or because of their X-ray emission,

* Based on observations obtained at the German-Spanish Astronomical Center, Calar Alto, operated by the Max-Planck-Institut für Astronomie, Heidelberg, jointly with the Spanish National Commission for Astronomy, on observations made at the 1.2 m telescope, located at Kryoneri Korinthias, and owned by the National Observatory of Athens, Greece, and on observations made with the OGS telescope, operated on the island of Tenerife by the European Space Agency, in the Spanish Observatorio del Teide of the IAC.

** Table 1 is only available in electronic form at <http://www.edpsciences.org>

with a strong dominance of dwarf novae and classical novae in the first group and magnetic CVs in the second group (Gänsicke 2005). It is therefore clear that CVs characterised by infrequent outbursts and/or low-amplitude variability, as well as lacking strong X-ray emission, will be underrepresented in the currently known CV population. Hypothetically, such objects could make up for the large number of predicted short-period CVs with low mass transfer rates.

We are currently carrying out a spectroscopic survey of CV candidates with the aim to produce a homogeneously selected sample of CVs that overcomes the observational biases mentioned above. In this paper, we describe the status of our survey, the identification of four new CVs with periods close to 4 h, and discuss the nature of CVs in the 3–4 h period range.

2. CVs in the Hamburg Quasar Survey

The primary purpose of our project to identify new CVs in the Hamburg Quasar Survey (HQS) is to establish a large homogeneously selected sample of systems that overcomes previous observational biases and that can subsequently be used to test our understanding of CV evolution (Gänsicke et al. 2002b). The HQS, an objective-prism survey, was carried out with the 0.8 m Schmidt telescope at Calar Alto Observatory to search for bright quasars in the northern sky at high galactic latitudes, $\delta > 0^\circ$ and $|b| > 20^\circ$, covering $\approx 13\,600 \text{ deg}^2$, with a dynamic range of $13 \lesssim B \lesssim 18.5$ (Hagen et al. 1995). The photographic plates cover a spectral range of $\sim 3400\text{--}5400 \text{ \AA}$ with a resolution of $\sim 45 \text{ \AA}$ at $H\beta$.

Our CV candidate selection made use of a property that has never been systematically exploited before: the *spectroscopic* hallmark of CVs, i.e. the presence of noticeable emission lines in most CVs. The CV candidate selection was carried out by visually inspecting 48 708 HQS prism spectra for the presence of Balmer emission lines. In order to test the efficiency of this method, we applied the same procedure to the subset of 84 previously known CVs (Downes et al. 2001, as of July 2001) that are contained in the HQS spectral data base. We positively recovered $\approx 90\%$ of the known short-period ($P_{\text{orb}} < 2 \text{ h}$) CVs, including prominent dwarf novae such as SW UMa or T Leo (the latter one has a rather long outburst cycle of $\sim 420 \text{ d}$), as well as magnetic CVs, such as AN UMa or ST LMi. The fraction of recovered systems drops to $\approx 40\%$ for long-period systems, with the largest fraction of missed identifications being nova-like variables with weak or no Balmer emission lines. In total, 62% of the previously known CVs with an HQS prism spectrum were positively identified by our selection method. We concluded from this test that the HQS should be very efficient in finding CVs below the period gap, as long as they have similar spectroscopic properties to the previously known systems, i.e. Balmer emission lines with equivalent widths $> 10 \text{ \AA}$ in $H\beta$. The decrease in detection efficiency for long-period systems has been compensated to some extent by follow-up programs investigating hot stars in the HQS, delivering a number of new CVs with weak emission lines (Heber et al. 1991).

In total, 53 new CVs were identified within this project, and substantial observational effort was invested in determining the properties of these systems. To date, 42 HQS CVs have

had their orbital period measured. Despite its good sensitivity for short-period CVs, only a small number of new short-period CVs have been found, and those that have been found fully confirm the expected properties: low-amplitude variability and/or long outburst recurrence times, e.g. KV Dra (HS 1449+6415, Nogami et al. 2000), HS 2331+3905 (Araujo-Betancor et al. 2005a), DW Cnc (HS 0756+1624, Rodríguez-Gil et al. 2004a), or HS 2219+1824 (Rodríguez-Gil et al. 2005a). The majority of the newly identified systems have orbital periods above the 2–3 h period gap, including rarely outbursting dwarf novae such as GY Cnc (HS 0907+1902, Gänsicke et al. 2000) or RX J0944.5+0357 (HS0941+0411, Mennickent et al. 2002); magnetic CVs with relatively weak X-ray emission, such as 1RXS J062518.2+733433 (HS0618+7336, Araujo-Betancor et al. 2003), RX J1554.2+2721 (HS 1552+2730, Thorstensen & Fenton 2002; Gänsicke et al. 2004b), and HS 0943+1404 (Rodríguez-Gil et al. 2005b); and half a dozen new SW Sextantis stars (Gänsicke et al. 2002c; Szkody et al. 2001; Rodríguez-Gil et al. 2004b; Rodríguez-Gil 2005).

While a full discussion of the implications that our search for CVs in the HQS has for our understanding of the galactic CV population has to await characterisation of the full HQS CV sample, an important preliminary statement that will not substantially change is: *there is no large population of nearby short-period CVs that resemble the known template systems*. Phrased differently, if the large population of short period CVs predicted by theory exists, the majority of these systems must look different from the known short-period systems, i.e. have weak emission lines and/or substantially redder continua. Interestingly, the Sloan Digital Sky Survey (SDSS) is discovering a number of CVs with a steep Balmer decrement, in which the white dwarf dominates the optical emission, a clear sign of low mass transfer rates (Szkody et al. 2005, and references therein). However, most of these systems are very faint, $g \approx 19\text{--}20$, implying that they are distant ($d > 100 \text{ pc}$) and not intrinsically numerous anywhere near the numbers predicted by theory.

An unexpected finding of our search for CVs in the HQS has been the identification of a large number of systems with orbital periods in the range 3–4 h. Here, we report the discovery of four additional CVs in that period range, HS 0139+0559, HS 0229+8016, HS 0506+7725, and HS 0642+5049. Despite being close in orbital period, these systems differ dramatically in their observed characteristic, and we discuss in detail the properties of the known CVs in the 3–4 h period range.

3. Observations and data reduction

3.1. Spectroscopy

An identification spectrum of HS 0139+0559 (see finding chart in Fig. 1) was obtained in October 1989 at the Calar Alto 3.5 m telescope using the Boller&Chivens spectrograph equipped with a 120 \AA/mm grating as part of a program to find blue stars (Heber et al. 1991). This spectrum (Fig. 2) is characterised by a blue continuum with strong absorption lines of the Balmer series, as well as of $\text{He I } \lambda 4471$. The absorption profiles have a rectangular shape with a full width at zero intensity (FWZI)

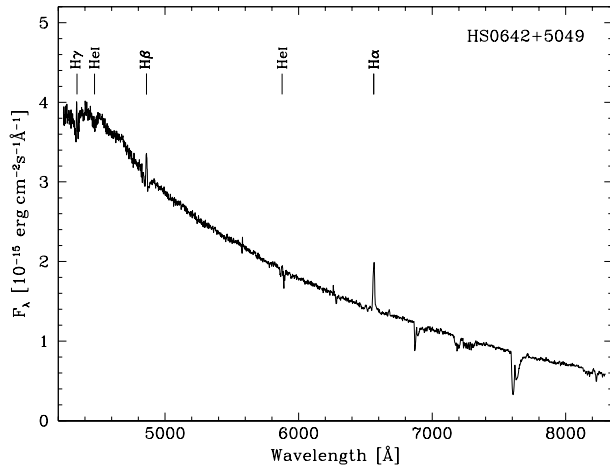


Fig. 5. Average of the 17 CAFOS G-100 spectra of HS 0642+5049 obtained at the Calar Alto 2.2 m telescope on October 24, 2004.

The $\lambda\lambda 4630$ – 4650 N/C Bowen blend and the $\text{He II } \lambda 4686$ emission lines are also detected. The strength of these high-ionisation lines is typical of novalike variables, magnetic CVs, or nova remnants.

HS 0642+5049 (Fig. 1) was spectroscopically identified as a CV on March 7, 1999, with CAFOS at the Calar Alto 2.2 m telescope. The spectrum of HS 0642+5049 (Fig. 5) contains a blue continuum with moderately strong $\text{H}\alpha$ emission. The $\text{H}\beta$ and $\text{H}\gamma$ emission is embedded in broad absorption troughs, and weak $\text{He I } \lambda 4471$ absorption is also detected. No $\text{He II } \lambda 4686$ and $\lambda\lambda 4630$ – 4650 N/C Bowen blend are detected.

In order to determine the orbital periods of HS 0139+0559, HS 0229+8016, HS 0506+7725, and HS 0642+5049, we obtained time-resolved spectroscopy at Calar Alto Observatory and Roche de los Muchachos Observatory throughout the period October 2002 to October 2004 (Table 1). At the Calar Alto 2.2 m telescope, we used the CAFOS spectrograph equipped with the G-100 grating and a $2\text{k} \times 2\text{k}$ pixel SITe CCD. This setup, in conjunction with a $1.2''$ slit, provided a spectral resolution of $\sim 4.1 \text{ \AA}$ (full width at half maximum, *FWHM*) covering the range 4240 – 8300 \AA . We used the double-armed TWIN spectrograph at the Calar Alto 3.5 m telescope equipped with the T05 grating in the blue and the T06 grating in the red, providing a spectral resolution of $\sim 1.2 \text{ \AA}$ (*FWHM*) in the ranges $\lambda\lambda 3810$ – 4940 and $\lambda\lambda 6440$ – 7510 . At the 2.5 m Isaac Newton Telescope (INT), we used the Intermediate Dispersion Spectrograph (IDS) equipped with the R632V grating and the $2\text{k} \times 4\text{k}$ pixel EEV10a detector. Using a slit width of $1.5''$ this setup provided a useful wavelength of ~ 4400 – 6800 \AA and a spectral resolution of $\sim 2.3 \text{ \AA}$. Arc calibration spectra were interleaved with the target observations every ~ 40 min.

In total, we obtained 55 spectra of HS 0139+0559, 74 spectra of HS 0229+8016, 86 spectra of HS 0506+7725, and 87 spectra of HS 0642+5049 (Table 1). Reduction of the follow-up spectroscopy consisting of bias and flat-field corrections and optimal extraction (Horne 1986) was carried out in IRAF.¹ The wavelength calibration of the extracted spectra was

¹ IRAF is distributed by the National Optical Astronomy Observatories.

performed in MOLLY. The dispersion relation was obtained by fitting a low-order polynomial to the arc lines, with the rms less than one tenth of the dispersion in all cases. The flexure of the telescope was accounted for by interpolating between the two arc exposures bracketing the target spectra.

The time-resolved spectra of HS 0139+0559 and HS 0229+8016 are similar to the identification spectra shown in Figs. 2 and 3 (bottom panel), with $\text{H}\beta$ and $\text{H}\gamma$ in absorption for most of the time and occasionally showing signs of emission cores. However, the G-100 spectra cover $\text{H}\alpha$ as well, which is observed in emission throughout, with low equivalent widths in the range 3 – 6 \AA . The time-resolved spectra of HS 0506+7725 are very similar to the identification spectrum shown in Fig. 4, with the difference of having no $\text{He II } \lambda 4686$ emission. The $\text{H}\alpha$ emission line has an average equivalent width of $\sim 15 \text{ \AA}$. The time-resolved spectra of HS 0642+5049 show $\text{H}\alpha$ in emission with an average equivalent width of $\sim 5 \text{ \AA}$, and weak $\text{H}\beta$ and $\text{H}\gamma$ emission embedded in broad absorption lines (Fig. 5).

3.2. Photometry

The spectroscopy of the four new cataclysmic variables was supplemented by differential CCD photometry obtained at six different telescopes (Table 1). Brief descriptions of the instrumentation used and the data reduction techniques are given below.

Braeside Observatory. Differential *B* and *R* photometry of HS 0139+0559 was obtained in December 1999/January 2000 at Braeside Observatory using the 0.41 m reflector together with an SITE 512×512 pixel CCD camera. The raw images were bias-subtracted, dark current-subtracted, and flat-fielded in a standard manner.

Kryoneri Observatory. We obtained differential *R*-band photometry of HS 0229+8016 (September 19 and 20, 2002) and HS 0506+7725 (October 8, 2002) at Kryoneri Observatory using the 1.2 m telescope equipped with a Photometrics SI-502 516×516 pixel CCD camera. The data were reduced using the pipeline described in Gänsicke et al. (2004a), which pre-processes the raw images in MIDAS and extracts aperture photometry using the SExtractor (Bertin & Arnouts 1996). The instrumental magnitudes of HS 0229+8016 were converted into apparent magnitudes using the comparison star labelled “C1” in Fig. 1 (USNO-A2.0 1650-00512682, $R = 12.6$). We found a mean magnitude of $R \approx 14.3$ during both nights. The apparent magnitudes of HS 0506+7725 were computed using the comparison star “C2” (USNO-A2.0 1650-00942250, $R = 13.1$), and an average magnitude of $R \approx 15.2$ was found.

Tuorla Observatory. We used the 0.7 m Schmidt-Vaisala telescope at Tuorla Observatory, equipped with an SBIG ST-8 CCD camera to obtain filterless photometry of HS 0229+8016 (January 10, 2003), HS 0506+7725 (January 4, 6, and 16, 2003), and HS 0642+5049 (December 30, 2003 and January 1,

2004). The reduction of the observations was carried out in the same way as described for the Kryoneri data. Using the same comparison stars as above, we found the mean magnitudes of HS 0229+8016 and HS 0506+7725 to be ≈ 14.3 and ≈ 15.8 , respectively. The apparent magnitudes of HS 0642+5049 were extracted using the comparison star “C3” in Fig. 1 (USNO-A2.0 1350-06806656, $R = 12.4$), and gave a mean magnitude of ≈ 15.5 .

Observatorio del Teide. At the Observatorio del Teide on Tenerife, we used the 1 m Optical Ground Station (OGS) and the 0.82 m IAC80 telescopes to obtain CCD photometry of HS 0506+7725 and HS 0642+5049. The telescopes were equipped with Thomson $1k \times 1k$ pixel CCD cameras. On November 15, 2003, the OGS was used to obtain differential photometry of HS 0506+7725 in white light. The data were taken using 2×2 binning and windowing to improve the time resolution. The images were bias and flat-field corrected and aligned within IRAF. Instrumental magnitudes of the CV and the comparison star “C2” were then extracted using the point spread function (PSF) photometry tasks package within IRAF. We found the mean magnitude of HS 0506+7725 during that night to be ≈ 14.6 . On December 1, 6, 7, and 8, 2004, we used the IAC80 telescope to obtain filterless photometry of HS 0642+5049. In order to achieve a high time resolution, windowing and binning 2×2 were applied. The data were reduced using MIDAS in the same manner as described for the Kryoneri run. The apparent magnitudes were extracted using the comparison star “C3”, resulting in a mean magnitude of ≈ 15.3 .

Calar Alto Observatory. During January 2003 and October 2004, we used CAFOS with the SITe $2k \times 2k$ pixel CCD camera on the 2.2 m telescope to obtain filterless differential photometry of HS 0506+7725 and HS 0642+5049 when the atmospheric conditions were too poor for spectroscopy. Only a small part of the CCD was read out in order to improve the time resolution. The data were reduced in an analogous fashion to the one described for the Kryoneri observations above. The mean magnitudes of HS 0506+7725 and HS 0642+5049 were found to be ≈ 14.9 and ≈ 15.6 , respectively.

Light curve morphology. The light curves of HS 0139+0559 (Fig. 6) and HS 0229+8016 (Fig. 7) display very little variability on nightly time scales, with amplitudes ≤ 0.02 mag and ~ 0.05 mag, respectively. In the case of HS 0229+8016, a low-amplitude modulation with a period of ~ 4 h is consistently detected during the two longest observations. HS 0506+7725 exhibits short-period variability with an amplitude of ~ 0.2 – 0.4 mag, which appear to be quasi-periodic oscillations on time scales of ~ 10 – 20 min (Fig. 8). No clearly repeating variation is detected on time scales of several hours (i.e. a putative orbital modulation). The light curves of HS 0642+5049 from the IAC80 (Fig. 9) show modulation with a period of ~ 3.5 h, which we interpret as the orbital period of the system. No substantial flickering activity is detected.

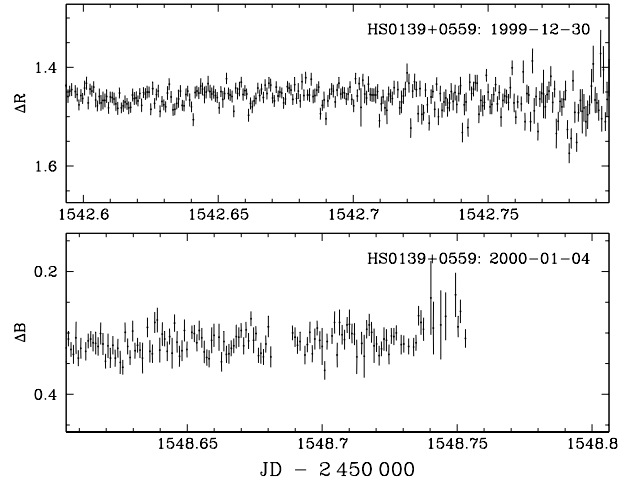


Fig. 6. Differential CCD R -band (*top panel*) and B -band (*bottom panel*) photometry of HS 0139+0559 obtained at the Braeside observatory.

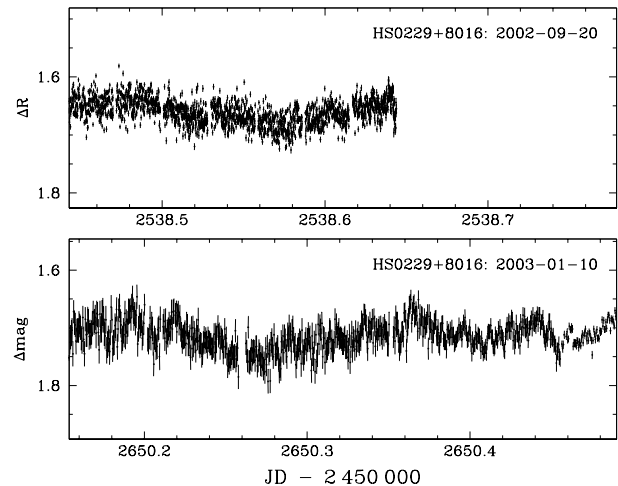


Fig. 7. Sample light curves of HS 0229+8016. *Top panel:* R -band data obtained at the Kryoneri observatory. *Bottom panel:* filterless data obtained at the Tuorla observatory.

The USNO-A2.0 catalogue lists HS 0139+0559 with $B = R = 14.4$, and we found $V \approx 15.4$ and $B \approx 14.9$ in our observations. HS 0229+8016 has $B = 13.9$ and $R = 13.8$ in the USNO-A2.0 catalogue, and it was found during our observations mostly near $B \approx V \approx 14.0$ – 14.6 , except on one occasion (August 1992) when it was as faint as $V \approx 15.0$ mag. HS 0506+7725 is listed with $B = 15.3$ and $R = 15.6$ in the USNO-A2.0 catalogue, and our data provides evidence of long-term variability of the mean magnitude by ~ 1 mag, but it dropped on one occasion (October 1995) into a deep low state at $B \approx 18.3$. HS 0642+5049 is found in the USNO-A2.0 catalogue with $B = 16.6$ and $R = 16.9$, and we found $V \approx 15.3$ – 15.5 mag without significant long-term variability of the system.

Table 2. Sine fits to the $H\alpha$ emission line radial velocities. The methods employed were a convolution with a single Gaussian (SG) or Schneider & Young’s (1980) double-Gaussian prescription (DG).

Object	Method	$FWHM/Sep.$ (km s^{-1})	T_0	Period (days)	K (km s^{-1})	γ (km s^{-1})
HS 0139+0559	SG	600	2452998.985 ± 0.013	0.16923 ± 0.00034	84.4 ± 4.8	18.4 ± 3.5
HS 0229+8016	SG	600	2452992.457 ± 0.006	0.161493 ± 0.000034	179.0 ± 5.2	35.5 ± 3.5
HS 0506+7725	DG	700/1500	2452990.679 ± 0.022	0.14770 ± 0.00014	42.6 ± 4.4	-66.7 ± 3.0

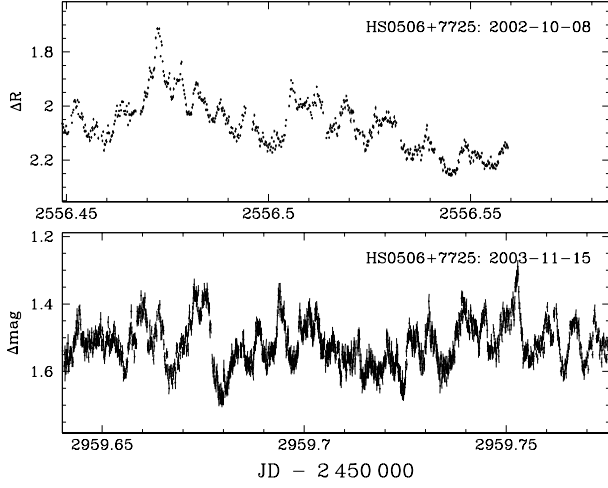


Fig. 8. Sample light curves of HS 0506+7725. *Top panel:* R -band data obtained at the Kryoneri observatory. *Bottom panel:* filterless data obtained at the OGS telescope.

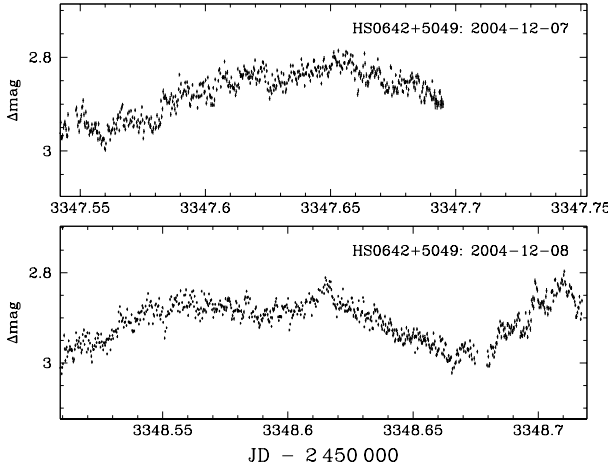


Fig. 9. Sample filterless light curves of HS 0642+5049 obtained at the IAC80 telescope.

4. Analysis

4.1. HS 0139+0559

In order to determine the orbital period of HS 0139+0559 we measured the radial velocity variations of $H\alpha$ by convolving the observed line profiles with a single Gaussian of $FWHM = 600 \text{ km s}^{-1}$. The spectra were continuum-normalised prior to this analysis. A Scargle (1982) period analysis of the radial velocity measurements was performed using the MIDAS/TSA context. The resulting periodogram (Fig. 10) shows a strong signal at $5.909 \pm 0.012 \text{ d}^{-1}$ surrounded by one-day aliases,

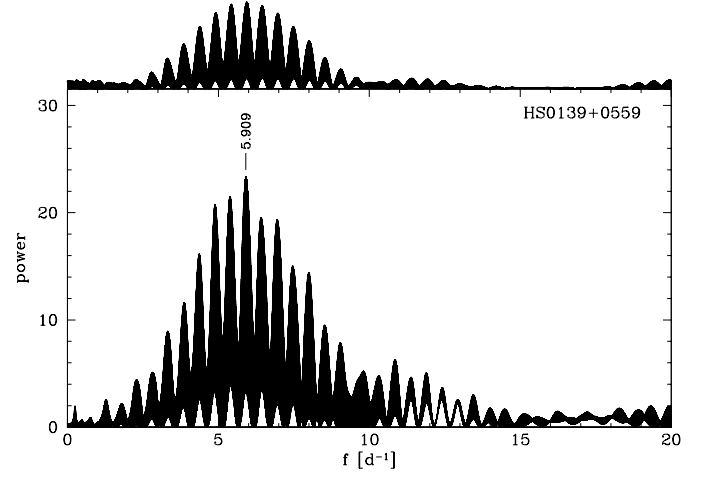


Fig. 10. The Scargle periodogram of the radial velocities of HS 0139+0559 measured from the $H\alpha$ emission line. The periodogram from a set of fake radial velocities is shown in the *top panel*.

where the error is determined from fitting a sine wave to the radial velocity variation (see Table 2 for the full fit parameter). In order to test the significance of the detected signal, we created a set of fake radial velocities by evaluating a sine function with a frequency of 5.909 d^{-1} at the exact times of the observed spectroscopic data. The amplitude of the sine wave was adjusted to reflect the observed radial velocity amplitude, and the fake radial velocity measurements were randomly offset from the computed sine wave using the observed errors. The periodogram of the fake data reproduces the alias structure of the periodogram computed from the observations very well. We conclude that the orbital period of HS 0139+0559 is $P_{\text{orb}} = 243.69 \pm 0.49 \text{ min}$. Folding the radial velocity measurements over that period results in a quasi-sinusoidal radial velocity curve with an amplitude of $84.4 \pm 4.8 \text{ km s}^{-1}$ (Fig. 14, top panel).

For completeness, we also used the Braeside B and R band photometry for a period analysis. As suggested by the flat light curve (Fig. 6), no significant signal is detected in the Scargle periodogram.

4.2. HS 0229+8016

An analogous radial velocity analysis as described in the previous section was carried out for HS 0229+8016. Inspection of the Scargle periodogram (Fig. 11) shows a somewhat more complex alias structure as a result of the inhomogeneous spacing of the spectroscopic observations. The strongest signal is found at $6.1922 \pm 0.0013 \text{ d}^{-1}$, where the error is again

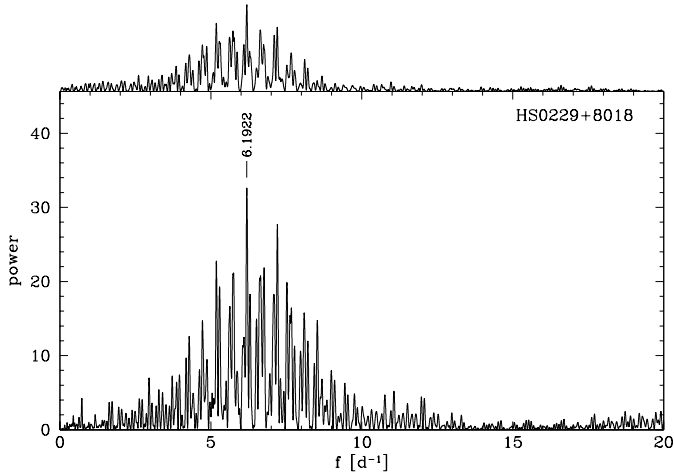


Fig. 11. The Scargle periodogram of the radial velocities of HS 0229+8016 measured from the $H\alpha$ emission line. The periodogram from a set of fake radial velocities is shown in the *top panel*.

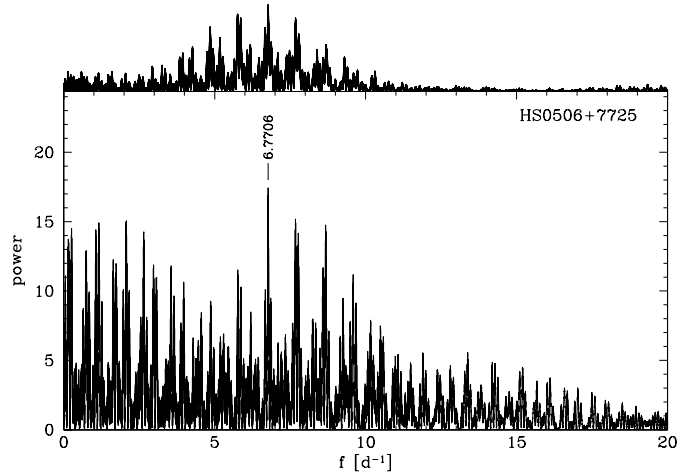


Fig. 12. The Scargle periodogram of the radial velocities of HS 0506+7725 measured from the $H\alpha$ emission line by using the double Gaussian method. The periodogram from a set of fake radial velocities is shown in the *top panel*.

computed from a sine fit to the radial velocity data (Table 2), and a fake data set computed using this frequency reproduces the overall alias structure well. We conclude that the most likely value for the orbital period of HS 0229+0559 is $P_{\text{orb}} = 232.550 \pm 0.049$ min. The phase-folded radial velocity curve shows quasi-sinusoidal modulation with an amplitude of 179.0 ± 5.2 km s^{-1} (Table 2).

Scargle periodograms computed from the two longest photometry runs on HS 0229+0559 are dominated by a broad signal near 5.2 d^{-1} (Kryoneri data) and 6.2 d^{-1} (Tuorla), which are consistent with the spectroscopic period or its one-day alias. While our photometric data is not sufficient to improve the period determination of HS 0229+0559, it suggests that the orbital period of HS 0229+0559 can be refined by a sequence of sufficiently long photometric time-series.

4.3. HS 0506+7725

Our initial analysis of the HS 0506+7725 $H\alpha$ radial velocity variation was carried out by applying a single-Gaussian convolution on the continuum-normalised line profiles. However, the Scargle periodogram computed from the measured radial velocity variations turned out to be dominated by a variety of signals in the range $\sim 1\text{--}5$ d^{-1} , none of which resulted in a plausible phase-folded radial velocity curve. In a second attempt, we applied the double Gaussian method of Schneider & Young (1980), using a Gaussian $FWHM = 700$ km s^{-1} and a separation of 1500 km s^{-1} to measure the radial velocity variation of the line wings. The Scargle periodogram resulting from these radial velocity measurements includes several peaks in the range $5\text{--}9$ d^{-1} (Fig. 12). The strongest signal is found at 6.7706 ± 0.0065 d^{-1} , which we identify as the likely orbital period of HS 0506+7725, $P_{\text{orb}} \approx 212.7 \pm 0.2$ min, where the error is determined from a sine fit to the radial velocity data (Table 2). The Scargle periodogram computed from a fake data set results in a much cleaner periodogram than the one obtained from the observed data, suggesting that the line wings are affected by additional velocity contributions apart from the

orbital motion. The $H\alpha$ radial velocities folded over the orbital period (Fig. 14) display a low amplitude of 42.6 ± 4.4 km s^{-1} and a relatively large amount of scatter, again suggesting that the orbital motion measured from the line wings is contaminated by another velocity component.

Our time-series analysis of the photometry of HS 0506+7725 did not lead to the detection of any significant signal, either at long (orbital) or at short (putative white dwarf spin) frequencies, making the observed short-term variability (Fig. 8) a nice example of non-coherent CV flickering.

4.4. HS 0642+5049

The 87 available spectra of HS 0642+5049 were subjected to radial velocity studies as outlined above, both using the single-Gaussian and double-Gaussian convolution techniques. None of the resulting Scargle periodograms contained any significant signal. Inspecting trailed spectra assembled from our data, we concluded that HS 0642+5049 does not show any radial velocity variation at our spectral resolution.

Considering the ~ 3.5 h modulation observed in the HS 0642+5049 light curves, we used the three longest and closest spaced photometric data sets obtained at the Calar Alto 2.2 m telescope (October 25, 2004) and the IAC80 (December 8 and 9, 2004) to determine the orbital period of the system. The strongest peak detected in the Scargle periodogram computed from these data is found at 6.3746 ± 0.0065 d^{-1} , surrounded by one-day aliases (Fig. 13). In order to test the significance of the signal, we created a set of fake data from a sine wave with a frequency of 6.3746 evaluated at the exact times of the observations. The alias structures of the periodograms calculated from the fake data and the real data agree well. We conclude that the orbital period of HS 0642+5049 is $P_{\text{orb}} \approx 225.90 \pm 0.23$ min.

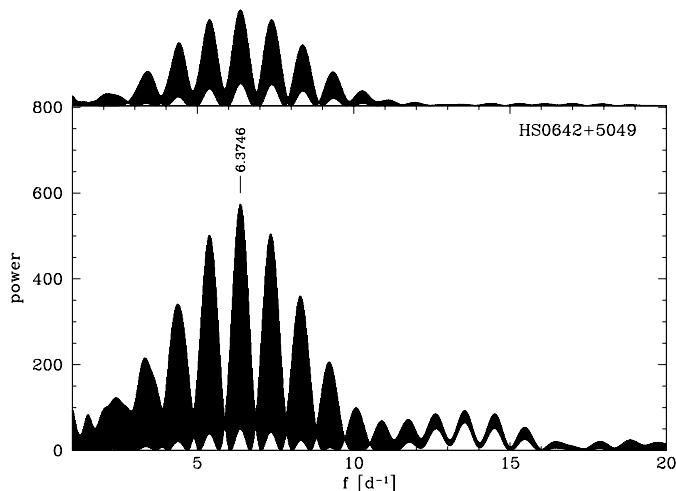


Fig. 13. The Scargle periodogram of HS 0642+5049 computed from the three longest nights of differential photometry obtained at the Calar Alto (October 25, 2004) and the IAC80 (December 8 and 9, 2004). The periodogram from a fake data set assuming a period of 225.90 min is shown in the *top panel*.

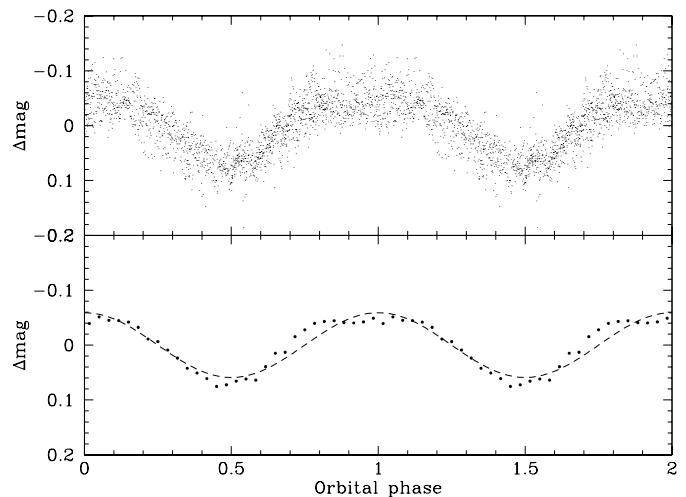


Fig. 15. HS 0642+5049 photometric data from the CAFOS (October 9, 2004) and the IAC80 (December 8 and 9, 2004) folded on $P_{\text{orb}} = 225.90$ min (*top panel*). The average light curve, binned into 30 phase, is shown in the *bottom panel* along with a sine fit (dashed line).

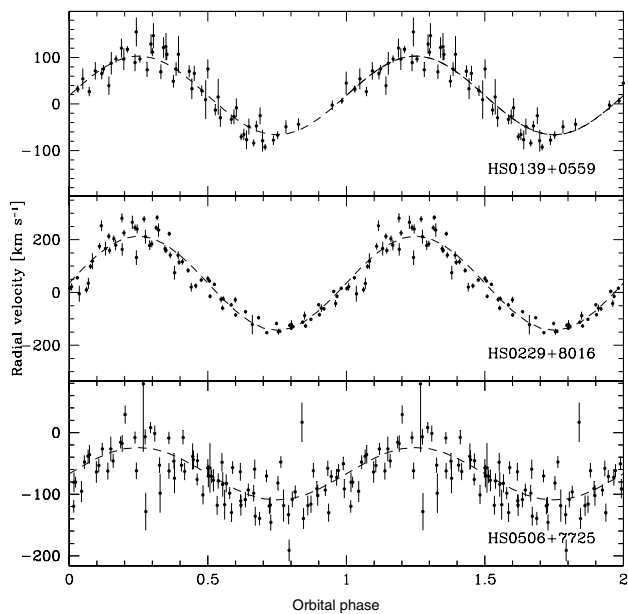


Fig. 14. $H\alpha$ radial velocities of HS 0139+0559 (*top panel*), HS 0229+8016 (*middle panel*), and HS 0506+7725 (*bottom panel*) folded on the period of 243.69 min, 232.550 min, and 212.7 min, respectively. The dashed lines are the best sine fits to the folded velocities.

Figure 15 shows the CAFOS and the IAC80 photometry folded on 225.90 min and averaged into 30 phase bins, which reflects the morphology of the individual light curves (Fig. 9).

5. Discussion

5.1. The inventory of the 3–4 h orbital period range

The primary aim of our search for CVs in the HQS is to establish the orbital periods and CV subtypes for a large

sample of CVs that were selected in a homogeneous way based on their spectroscopic properties. The properties of this sample will then be compared with the predictions of CV evolution theory. Here, we report the spectroscopic identification and detailed follow-up studies of HS 0139+0559, HS 0229+8016, HS 0506+7725, and HS 0642+5049, which have the orbital periods of 243.69 min, 232.550 min, 212.7 min, and 225.90 min, respectively. This follows the trend noticed by Gänsicke et al. (2002b) and, more recently, by Gänsicke (2004) and Rodríguez-Gil (2005) that the majority of the new CVs identified in the HQS have orbital periods above the period gap and the bulk of them are concentrated in the 3–4 h orbital period range. Currently, orbital periods have been determined for 42 systems out of a total of 53 new HQS CVs, and Fig. 16 compares the period distribution of these new HQS CVs with the period distribution of the CVs from the Ritter & Kolb catalogue (2003, V7.4). Even though the follow-up of the new HQS CVs is not yet complete, it is already now clear that our survey *did not* identify the large number of short-period CVs predicted by the population models (e.g. Kolb 1993; Howell et al. 1997), even though our selection method (= detection of Balmer emission lines) is best suited for the identification of low mass transfer systems that might be inconspicuous in other ways (variability, X-rays), such as the short-period dwarf novae HS 1449+6415 (Nogami et al. 2000) and HS 2219+1824 (Rodríguez-Gil et al. 2005a), or the ultra-short period HS 2331+3905, which might be a WZ Sge-type dwarf novae with extremely long outburst recurrence times (Araujo-Betancor et al. 2005a). The (somewhat preliminary) conclusion is that, if a large number of short-period CVs does indeed exist, they must look different from the well-known examples such as WZ Sge.

The HQS CV survey has been very prolific in identifying relatively bright long-period CVs with a distinct preference for the 3–4 h period range (Fig. 16), including the four

Table 3. Comparison of the observational characteristics of the four new CVs. The (non)detection of X-ray emission refers to the ROSAT All Sky Survey (Voges et al. 2000). The CV subtypes are abbreviated as UX = UX UMa type novalike variable, ZC = ZCam type dwarf nova, VY = VY Scl star.

Object	P_{orb} [min]	Radial velocity variation	Photometric variability			X-ray	type
			Orbital	Flickering	Long-term		
HS 0139+0559	243.7	clean, moderate amplitude	none	none	none	no	UX or ZC
HS 0229+8016	232.6	clean, large amplitude	very low amplitude	none	~1.3 mag	no	UX or ZC
HS 0506+7725	212.7	scatter, low amplitude	not obvious	large amplitude	~3 mag low state	yes	VY
HS 0642+5049	225.9	very low amplitude	moderate amplitude	low amplitude	none	maybe	UX or ZC

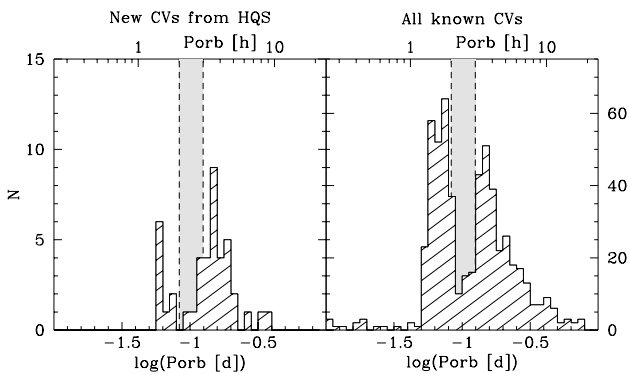


Fig. 16. The period distribution of 42 new CVs discovered in the HQS (left panel) and of all known CVs (right panel, from Ritter & Kolb 2003, V7.4). The 2–3 h period gap is shaded in gray.

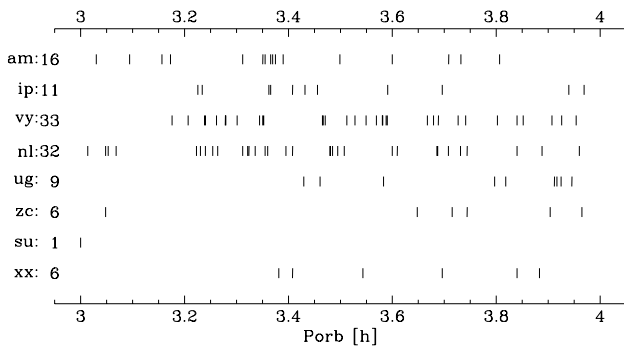


Fig. 17. The period distribution of the individual CV subtypes in the 3–4 h period range. From top to bottom: polars (am), intermediate polars (ip), VY Scl and SW Sex stars (vy), novalike variables and nova remnants that are neither VY Scl nor SW Sex stars (nl), U Gem type dwarf novae (ug), Z Cam type dwarf novae (zc), SU UMa type dwarf novae (su), and systems with undetermined CV subtype (xx).

new CVs presented in this paper. The majority of these new long-period CVs are weak or no X-ray emitters, and they display little long-term variability – in fact, only five confirmed dwarf novae are among the 28 new systems found above the gap. Gänsicke (2004) and Rodríguez-Gil (2005) pointed out the large number of SW Sextantis stars among the new HQS CVs, which represent 25% of all newly identified CVs above the gap, and nearly half of all the new CVs in the 3–4 h period range. For comparison, we show in Fig. 17 the inventory of the 3–4 h orbital period range according to

Ritter & Kolb (2003, V7.4). We find that 114 CVs (20% of all CVs with known P_{orb}) inhabit the 3–4 h period range, of which 27 (24%) are confirmed magnetic systems (intermediate polars, polars). 33 (29%) belong to the group of either VY Scl or SW Sex stars, which share similar properties, and are suspected to contain magnetic white dwarfs as well (e.g. Rodríguez-Gil et al. 2001; Hameury & Lasota 2002). While the ratio of definite magnetic CVs in the 3–4 h period range (24%) is already very high compared to the incidence of magnetism in isolated white dwarfs (Liebert et al. 2003), confirmation of significant magnetism in the white dwarfs in VY Scl/SW Sex stars would raise the ratio of magnetic/non-magnetic CVs well above 50%, which conflicts with any of the current models of CV evolution. Whatever the verdict on the magnetic fields in VY Scl/SW Sex stars will be, the large number of CVs belonging to this type suggests that they represent an important phase of CV evolution rather than some unusual combination of their physical properties. For completeness, 32 (28%) novalike variables that do not belong to either the VY Scl or SW Sex class populate the 3–4 h period range². While a number of those systems definitely do not share any of the VY Scl/SW Sex properties, a fair fraction of these systems has been studied only in a very limited way, and hence some of them might well join the VY Scl/SW Sex class upon more detailed scrutiny. Finally, 16 (14%) dwarf novae are known in the 3–4 h period range, and the scarcity of systems undergoing thermal disc instabilities just above the period gap is a well-known fact (e.g. Shafter et al. 1986; Shafter 1992).

5.2. The nature of the four new CVs

Based on observational characteristics (summarised in Table 3) we discuss the likely nature of the four new CVs.

HS 0506+7725 shows short time scale flickering with quasi-periodic oscillations on time scales of ~15 min. The relatively narrow emission lines and the low amplitude of the radial velocity variations suggest a low inclination. The system has been detected in the RASS (Voges et al. 2000) at 0.07 cts s^{-1} (1RXS J051336.1+772836) with a hard spectrum, and has been previously detected as an X-ray source by EINSTEIN (2E 0506.1+7725). The presence of moderately

² The classification of Ritter & Kolb (2003) is somewhat confusing, as their use of the UX UMa type disagrees with the more common definition of systems characterised by persistent broad Balmer absorption lines.

strong He II $\lambda 4686$ emission in the identification spectrum independently confirms the presence of ionising radiation in the system. The detection of a deep low state at $B \approx 18.3$ on one of the HQS prism plates clearly identifies the system as a VY Scl star. The system does not display evidence *at face value* of being an SW Sex star; but as it is obviously a low-inclination binary, a spectroscopic study at higher resolution would be useful to test for anomalous radial velocity behaviour in the emission lines.

The other three systems, HS 0139+0559, HS 0229+8016, and HS 0642+5049 are spectroscopically very similar, being characterised by thick-disc absorption line spectra. The fact that we have observed them on various occasions and found them always at nearly the same magnitude and with the same spectral properties³ makes it very unlikely that these systems are U Gem-type dwarf novae observed during outburst. While HS 0139+0559 and HS 0229+8016 are not detected in the RASS, a faint X-ray source is found near HS 0642+5049 (1RXS J066618.4+504601, 0.02 cts s⁻¹), which coincides within the 29'' position error of the RASS detection with the CV. The fact that there are no other nearby objects suggests that HS 0642+5049 is a weak X-ray emitter. None of the systems shows strong flickering activity. One puzzling difference among the three systems is that, whereas HS 0139+0559 and HS 0229+8016 show no or only very low-amplitude orbital photometric variability but exhibit clean quasi-sinusoidal radial velocity variations in their emission lines, HS 0642+5049 does not display any radial velocity variation but shows a 0.2 mag photometric modulation. It is very difficult to reconcile this opposite difference in spectroscopic/photometric behaviour in the simple picture of a high-mass transfer CV with a steady-state accretion disc. Based on our data, we identify all three systems either as UX UMa-type novalike variables or as Z Cam-type dwarf novae observed in periods of standstill. Optical long-term monitoring will be necessary to distinguish between these two possibilities.

6. Conclusions

We have identified HS 0139+0559, HS 0229+8016, HS 0506+7725, and HS 0642+5049 as long-period CVs with the orbital periods of 243.69 ± 0.49 min, 232.550 ± 0.049 min, 212.7 ± 0.2 min, and 225.90 ± 0.23 , respectively. HS 0506+7725 is a VY Scl novalike variable characterised by a strong emission-line spectrum. HS 0139+0559, HS 0229+8016, and HS 0642+5049 have thick-disc spectra and are either UX UMa type novalike variables or Z Cam dwarf nova. None of the objects is a strong X-ray source or displays large-amplitude outbursts, which underlines the strength of CV surveys on spectroscopically selected candidates.

³ With one exception: HS 0229+8016 was observed in August 1992 in a somewhat fainter state, $V \approx 15.0$, compared to its typical brightness near 14 mag. On that occasion, the Balmer and He I absorption lines were absent/weak, and the strength of the emission lines had markedly increased.

Acknowledgements. A.A. thanks the Royal Thai Government for a studentship. B.T.G. and P.R.G. were supported by a PPARC Advanced Fellowship and a PDRA grant, respectively. The HQS was supported by the Deutsche Forschungsgemeinschaft through grants Re 353/11 and Re 353/22. Tom Marsh is acknowledged for developing and sharing his reduction and analysis package MOLLY. We thank the referee, Mike Shara, for his comments that lead to an improved presentation of the paper.

References

- Andronov, N., Pinsonneault, M., & Sills, A. 2003, *ApJ*, 582, 358
 Araujo-Betancor, S., Gänsicke, B. T., Hagen, H.-J., Rodríguez-Gil, P., & Engels, D. 2003, *A&A*, 406, 213
 Araujo-Betancor, S., Gänsicke, B. T., Hagen, H.-J., et al. 2005a, *A&A*, 430, 629
 Araujo-Betancor, S., Gänsicke, B. T., Long, K. S., et al. 2005b, *ApJ*, 622, 589
 Barker, J., & Kolb, U. 2003, *MNRAS*, 340, 623
 Bertin, E., & Arnouts, S. 1996, *A&AS*, 117, 393
 de Kool, M. 1992, *A&A*, 261, 188
 Downes, R. A. 1986, *ApJ*, 307, 170
 Downes, R. A., Webbink, R. F., Shara, M. M., et al. 2001, *PASP*, 113, 764
 Gänsicke, B. T. 2004, in *Compact Binaries and Beyond*, ed. G. Tovmassian & E. Sion, *Rev. Mex. Astron. Astrofis., Ser. Conf.*, 20, 152
 Gänsicke, B. T. 2005, in *The Astrophysics of Cataclysmic Variables and Related Objects*, ed. J.-M. Hameury & J.-P. Lasota, *ASP Conf. Ser.*, 330
 Gänsicke, B. T., Fried, R. E., Hagen, H.-J., et al. 2000, *A&A*, 356, L79
 Gänsicke, B. T., Beuermann, K., & Reinsch, K. 2002a, *The Physics of Cataclysmic Variables and Related Objects*, *ASP Conf. Ser.*, 261
 Gänsicke, B. T., Hagen, H. J., & Engels, D. 2002b, in *The Physics of Cataclysmic Variables and Related Objects*, ed. B. T. Gänsicke, K. Beuermann, & K. Reinsch, *ASP Conf. Ser.*, 261, 190
 Gänsicke, B. T., Hagen, H.-J., Kube, J., et al. 2002c, in *The Physics of Cataclysmic Variables and Related Objects*, ed. B. T. Gänsicke, K. Beuermann, & K. Reinsch, *ASP Conf. Ser.*, 261, 623
 Gänsicke, B. T., Araujo-Betancor, S., Hagen, H.-J., et al. 2004a, *A&A*, 418, 265
 Gänsicke, B. T., Jordan, S., Beuermann, K., et al. 2004b, *ApJ*, 613, L141
 Hagen, H. J., Groote, D., Engels, D., & Reimers, D. 1995, *A&AS*, 111, 195
 Hameury, J. M., & Lasota, J. P. 2002, *A&A*, 394, 231
 Hameury, J.-M., & Lasota, J.-P. (eds.) 2005, *The Astrophysics of Cataclysmic Variables and Related Objects*, *ASP Conf. Ser.*, 330
 Heber, U., Jordan, S., & Weidemann, V. 1991, in *NATO ASIC Proc.*, 336, White Dwarfs, 109
 Horne, K. 1986, *PASP*, 98, 609
 Howell, S. B., Rappaport, S., & Politano, M. 1997, *MNRAS*, 287, 929
 King, A. R. 1988, *QJRAS*, 29, 1
 Kolb, U. 1993, *A&A*, 271, 149
 Liebert, J., Bergeron, P., & Holberg, J. B. 2003, *AJ*, 125, 348
 Mennickent, R. E., Tovmassian, G., Zharikov, S. V., et al. 2002, *A&A*, 383, 933
 Nogami, D., Engels, D., Gänsicke, B. T., et al. 2000, *A&A*, 364, 701
 Politano, M. 1996, *ApJ*, 465, 338
 Ringwald, F. A. 1996, in *Cataclysmic Variables and Related Objects*, ed. A. Evans & J. H. Wood (Dordrecht: Kluwer), *IAU Coll.*, 158, 89

- Ritter, H., & Burkert, A. 1986, *A&A*, 158, 161
- Ritter, H., & Kolb, U. 2003, *A&A*, 404, 301
- Rodríguez-Gil, P. 2005, in *The Astrophysics of Cataclysmic Variables and Related Objects*, ed. J.-M. Hameury & J.-P. Lasota, ASP Conf. Ser., 330, 335
- Rodríguez-Gil, P., Casares, J., Martínez-Pais, I. G., Hakala, P., & Steeghs, D. 2001, *ApJ*, 548, L49
- Rodríguez-Gil, P., Gänsicke, B. T., Araujo-Betancor, S., & Casares, J. 2004a, *MNRAS*, 349, 367
- Rodríguez-Gil, P., Gänsicke, B. T., Barwig, H., Hagen, H.-J., & Engels, D. 2004b, *A&A*, 424, 647
- Rodríguez-Gil, P., Gänsicke, B. T., Hagen, H.-J., et al. 2005a, *A&A*, 431, 269
- Rodríguez-Gil, P., Gänsicke, B. T., Hagen, H.-J., et al. 2005b, *A&A*, 440, 701
- Scargle, J. D. 1982, *ApJ*, 263, 835
- Schenker, K., & King, A. R. 2002, in *The Physics of Cataclysmic Variables and Related Objects*, ed. B. T. Gänsicke, K. Beuermann, & K. Reinsch, ASP Conf. Ser., 261, 242
- Schneider, D. P., & Young, P. 1980, *ApJ*, 238, 946
- Shafter, A. W. 1992, *ApJ*, 394, 268
- Shafter, A. W., Wheeler, J. C., & Cannizzo, J. K. 1986, *ApJ*, 305, 261
- Szkody, P., Gänsicke, B. T., Fried, R. E., Heber, U., & Erb, D. K. 2001, *PASP*, 113, 1215
- Szkody, P., Henden, A., Fraser, O. J., et al. 2005, *AJ*, 129, 2386
- Taam, R. E., Sandquist, E. L., & Dubus, G. 2003, *ApJ*, 592, 1124
- Thorstensen, J. R., & Fenton, W. H. 2002, *PASP*, 114, 74
- Voges, W., Aschenbach, B., Boller, T., et al. 2000, *IAU Circ.*, 7432

Online Material

Table 1. Log of the observations.

Date	UT time	Filter/ Grating	Exp. (s)	Frames	Mean mag
HS 0139+0559					
Spectroscopy: Calar Alto 3.5 m and B and C					
1989 Jan. 22	19:21	120 Å/mm	900	1	–
Spectroscopy: Calar Alto 3.5 m and TWIN					
2002 Oct. 28	23:53–00:03	T08/T01	300	1	–
2002 Oct. 29	22:36–03:21	T05/T06	600	16	–
Spectroscopy: Calar Alto 2.2 m and CAFOS					
2003 Dec. 24	18:25–00:10	G-100	600	27	≈15.4
2003 Dec. 26	18:34–20:48	G-100	600	12	≈15.1
Spectroscopy: Hamburg-Schmidt telescope at Calar Alto					
1981 Nov. 01	–	Prism	3600	1	≈14.9
1981 Nov. 02	–	Prism	3600	1	≈14.9
Photometry: Braeside Observatory					
1999 Dec. 30	02:15–07:04	R	70	293	–
2000 Jan. 04	02:31–06:04	B	50	136	–
HS 0229+8016					
Spectroscopy: Calar Alto 2.2 m and B and C					
1992 Aug. 08	03:16		900	1	≈15.0
Spectroscopy: Calar Alto 2.2 m and CAFOS					
1998 Oct. 05	01:37	B-200	1800	1	≈13.7
2003 Dec. 14	19:18–00:55	G-100	600	24	≈14.2
2003 Dec. 16	20:21–03:08	G-100	600	27	–
2003 Dec. 23	18:49–21:01	G-100	600	12	≈14.5
2003 Dec. 26	21:34–22:53	G-100	600	7	≈14.1
2003 Dec. 27	18:46–19:22	G-100	600	4	≈13.7
Spectroscopy: Hamburg-Schmidt telescope at Calar Alto					
1986 Nov. 05	–	Prism	3600	1	≈14.4
1986 Nov. 06	–	Prism	3600	1	≈14.2
1994 Nov. 12	–	Prism	3600	1	≈14.6
Photometry: Kryoneri Observatory					
2002 Sep. 20	01:30–03:28	R	5	840	≈14.2
2002 Sep. 20	22:37–03:27	R	5	1680	≈14.3
Photometry: Tuorla Observatory					
2003 Jan. 10	15:41–23:45	Clear	30	695	≈14.3
HS 0506+7725					
Spectroscopy: Calar Alto 3.5 m and TWIN					
2002 Dec. 03	03:22–05:09	T05/T06	600	10	–
Spectroscopy: Calar Alto 2.2 m and CAFOS					
1998 Feb. 02	19:43	B-400	180	1	–
2002 Dec. 09	00:19–00:30	G-100	600	2	≈15.4
2003 Dec. 13	23:25–03:53	G-100	600	23	≈14.7
2003 Dec. 15	01:34–06:13	G-100	600	23	≈14.9
2003 Dec. 17	03:40–05:57	G-100	600	12	–
2003 Dec. 23	22:19–00:31	G-100	600	12	≈14.9
2003 Dec. 26	02:52–03:28	G-100	600	4	≈14.9

Table 1. continued.

Date	UT time	Filter/ Grating	Exp. (s)	Frames	Mean mag
Spectroscopy: Hamburg-Schmidt telescope at Calar Alto					
1987 Oct. 29	–	Prism	3600	1	≈15.1
1994 Jan. 12	–	Prism	3600	1	≈15.3
1995 Oct. 23	–	Prism	3600	1	≈18.3
Photometry: Kryoneri Observatory					
2002 Oct. 08	22:46–01:25	R	10	599	≈15.2
Photometry: Tuorla Observatory					
2003 Jan. 04	16:13–20:16	Clear	120	32	≈15.7
2003 Jan. 06	15:47–20:46	Clear	60	213	≈15.8
2003 Jan. 16	20:18–22:40	Clear	60	115	≈15.9
Photometry: OGS					
2003 Nov. 15	03:21–06:37	Clear	5	1110	≈14.6
Photometry: Calar Alto 2.2 m and CAFOS					
2003 Jan. 01	01:01–03:24	V	30	85	≈15.1
2003 Dec. 16	00:05–05:11	Clear	15–30	346	≈14.8
2003 Dec. 25	19:15–02:29	Clear	15–30	296	≈14.9
2003 Dec. 27	04:03–06:16	Clear	20	149	≈14.9
2003 Dec. 27	20:33–23:55	Clear	20	288	≈14.8
HS 0642+5049					
Spectroscopy: Calar Alto 2.2 m and CAFOS					
1999 Mar. 07	19:11	B-400	300	1	–
2003 Apr. 27	20:03–21:53	G-100	600	9	≈15.6
2003 May 10	20:20–21:21	G-100	600	6	–
2003 May 11	20:17–21:20	G-100	600	6	–
2003 Dec. 25	00:56–05:35	G-100	600	24	≈15.5
2003 Dec. 27	02:50–03:01	G-100	600	2	≈15.3
2004 Oct. 24	02:12–05:26	G-100	600	17	≈15.3
2004 Oct. 26	04:25–05:31	G-100	600	7	≈15.4
Spectroscopy: INT 2.5 m and IDS					
2003 Apr. 25	21:21–22:14	R632V	600	6	–
2003 Apr. 26	21:17–21:49	R632V	600–900	4	–
2003 Apr. 28	21:15–22:08	R632V	600	6	–
Spectroscopy: Hamburg-Schmidt telescope at Calar Alto					
1991 Nov. 10	–	Prism	3600	1	≈15.8
1993 Oct. 24	–	Prism	3600	1	≈16.0
Photometry: Tuorla Observatory					
2003 Dec. 30	19:58–21:06	Clear	120	46	≈15.4
2004 Jan. 01	18:37–23:27	Clear	60	250	≈15.5
Photometry: Calar Alto 2.2 m and CAFOS					
2003 Dec. 26	04:20–06:14	Clear	20–30	149	≈15.6
2004 Oct. 22	04:01–05:25	Clear	15	59	≈15.7
2004 Oct. 25	01:42–05:51	Clear	10–15	463	≈15.5
Photometry: IAC80					
2004 Dec. 02	04:01–05:00	Clear	10	150	≈15.4
2004 Dec. 07	05:10–06:11	Clear	15	139	≈15.3
2004 Dec. 08	01:00–04:41	Clear	10	528	≈15.3
2004 Dec. 09	00:13–05:14	Clear	10	738	≈15.3